


Integration of quantitative diffusion kurtosis imaging and prostate specific antigen in differential diagnostic of prostate cancer

Weigen Yao, BM* , Jiaju Zheng, BM, Chunhong Han, BM, Pengcong Lu, BM, Lihua Mao, BM, Jie Liu, BM, GuiCha Wang, BM, Shufang Zou, BM, Lifeng Li, BM, Ying Xu, MM

Abstract

This study aimed to evaluate the diagnostic performance of diffusion kurtosis imaging (DKI) and prostate-specific antigen (PSA) biomarkers in differentiating prostate cancer (PCa) and benign prostatic hyperplasia (BPH).

A total of 43 cases of prostate diseases verified by pathology were enrolled in the present study. These cases were assigned to the BPH group ($n=20$, 68.85 ± 10.81 years old) and PCa group ($n=23$, 74.13 ± 7.37 years old). All patients underwent routine prostate magnetic resonance imaging and DKI examinations, and the mean diffusivity (MD), mean kurtosis (MK), and fractional anisotropy (FA) values were calculated. Three serum indicators (PSA, free PSA [fPSA], and f/t PSA) were collected. We used univariate logistic regression to analyze the above quantitative parameters between the 2 groups, and the independent factors were further incorporated into the multivariate logistic regression model. The area under the receiver operating characteristic curve (AUC) was used to evaluate the diagnostic efficacy of the single indicator and combined model.

The difference in PSA, f/t PSA, MK, and FA between PCa and BPH was statistically significant ($P < .05$). The AUC for the combined model (f/t PSA, MK, and FA) of 0.972 (95% confidence interval [CI]: 0.928, 1.000) was higher than the AUC of 0.902 (95% CI: 0.801, 1.000) for f/t PSA, 0.833 (95% CI: 0.707, 0.958) for MK, and 0.807 (95% CI: 0.679, 0.934) for FA.

The MK and FA values for DKI and f/t PSA effectively identify PCa and BPH, compared to the PSA indicators. Combining DKI and PSA derivatives can further improve the diagnosis efficiency and might help in the clinical setting.

Abbreviations: ADC = apparent diffusion coefficient, AUC = area under the receiver operating characteristic curve, BPH = benign prostatic hyperplasia, DKI = diffusion kurtosis imaging, DWI = diffusion-weighted image, FA = fractional anisotropy, fPSA = free PSA, MD = mean diffusivity, MK = mean kurtosis, MRI = magnetic resonance imaging, PCa = prostate cancer, PSA = prostate-specific antigen, ROI = region of interest, tPSA = total PSA, TRUS = transrectal ultrasonography.

Keywords: benign prostatic hyperplasia, diffusion kurtosis imaging, prostate cancer, prostate-specific antigen

Editor: Roxana Covali.

This study was funded by Medical and health Science and Technology Project of Zhejiang Province (Grant No. 2019KY638) and the Yuyao Science and Technology Project (Grant No: 2019YZD02).

This study was approved by the ethics committee of Yuyao People's Hospital; the informed consent requirement was waived.

The authors have no conflicts of interest to disclose.

The authors declare that all data supporting the findings of this study are available within the article.

All data generated or analyzed during this study are included in this published article [and its supplementary information files].

Department of Radiology, Yuyao People's Hospital, Yuyao, Zhejiang, China.

* Correspondence: Weigen Yao, Department of Radiology, Yuyao People's Hospital, 800 Chengdong Road, Yuyao, Zhejiang, 315400, China (e-mail: yyfsk123@163.com).

Copyright © 2021 the Author(s). Published by Wolters Kluwer Health, Inc. This is an open access article distributed under the terms of the Creative Commons Attribution-Non Commercial License 4.0 (CCBY-NC), where it is permissible to download, share, remix, transform, and buildup the work provided it is properly cited. The work cannot be used commercially without permission from the journal. <http://creativecommons.org/licenses/by-nc/4.0>

How to cite this article: Yao W, Zheng J, Han C, Lu P, Mao L, Liu J, Wang G, Zou S, Li L, Xu Y. Integration of quantitative diffusion kurtosis imaging and prostate specific antigen in differential diagnostic of prostate cancer. *Medicine* 2021;100:35(e27144).

Received: 29 October 2020 / Received in final form: 16 August 2021 /

Accepted: 18 August 2021

<http://dx.doi.org/10.1097/MD.00000000000027144>

1. Introduction

Prostate cancer (PCa) is the second most frequent malignant tumor worldwide, severely threatening people's health.^[1] The epidemiological data of PCa revealed that there are approximately 1.6 million cases and 0.366 million deaths annually, and the morbidity and mortality of PCa have gradually increased with the aging population and lifestyles in recent years.^[2,3] The therapeutic method of PCa is mainly hormone therapy, including surgical castration, pharmacological blockage of androgen production, and blockage of testosterone.^[4,5] The PCa and benign prostatic hyperplasia (BPH) have the same clinical symptoms; however, the treatment and prognosis are different. Hence, the accurate differential diagnosis of PCa and BPH is crucial for patients.

The gold standard method for predicting PCa and BPH is the histopathologic finding.^[6] Nevertheless, a needle biopsy may be biased due to tumor heterogeneity, and this may sometimes induce bleeding and injury to the vital tissues and organs, such as urinary retention and vasovagal response.^[7] Serum prostate-specific antigen (PSA) is the most common clinical test for PCa, and is used to monitor the aggressiveness of tumors. Some research has indicated that increasing serum PSA levels corresponds to the advanced TNM stage and poor outcomes.^[8] PSA can be secreted by prostate and PCa cells. Normally, due to the presence of the blood-epithelial barrier, only a small amount

of PSA enters the blood, and serum PSA levels are stable at low levels. When PCa occurs, serum PSA significantly increases. At the same time, the patient's age and prostate volume would also affect the serum PSA levels. Given the low specificity and diagnostic efficacy, many men without PCa also underwent unnecessary biopsies.^[9,10] A previous study demonstrated that only a quarter of men suffered from PCa with PSA between 4 and 10 ng/mL.^[9]

Magnetic resonance imaging (MRI) is a noninvasive imaging technology widely used in prostate clinical practice and is the preferred imaging strategy for diagnosing PCa.^[11] This can not only provide a highly defined anatomical image of the zonal architecture of the prostate gland with excellent soft-tissue contrast, but also provide more diagnostic information by multi-modal MRI imaging, which is superior to other imaging methods.^[12] Nevertheless, significant differences exist between different readers when facing PCa detection using the prostate imaging reporting and data system (PI-RADS) v2 system on conventional prostate MRI.^[13] Due to its definition, PI-RADS scoring can be affected by subjectivity and inter-/intra-operator variability.^[13] Recently, diffusion kurtosis imaging (DKI) has been considered a key method to investigate the diffusion of water molecules and detect the lesion microstructure. In general, the diffusion of water molecules presents an abnormal distribution due to the differences in structures and functions. Meanwhile, abnormal proliferation, necrocytosis, and fresh angiogenesis result in the alteration of microstructure in tumors.^[14] Therefore, DKI was employed to study tumor imaging phenotypes and biological behavior, directly correlated to tissue physiological and pathological characteristics.^[15] In the present study, the DKI quantitative method and serum indicators were combined to comprehensively evaluate PCa and BPH, which may be helpful to provide more accurate diagnosis and risk factor assessment information, and a reference for treatment.

2. Methods

2.1. Patient population

The present retrospective study was approved by the ethics committee of the Yuyao People's Hospital and the requirement for informed consent was waived. A total of 78 prostate patients confirmed by pathology at our hospital from December 2018 to June 2020 were collected. The inclusion criteria were: complete pretreatment prostate MRI DKI examination and laboratory data; pathological results obtained through rectal ultrasound or surgery; and 10-core prostate biopsy with pathological results performed in the next 2 weeks after DKI examination. The exclusion criteria were: poor DKI image quality, and malignant tumors in other parts of the body. Finally, a total of 43 patients were included in the present study. The serum indicators, pathological results, and MRI images of each case were collected. Based on pathological results, these patients were assigned to the BPH group ($n=20$, 68.85 ± 10.81 years old) and PCa group ($n=23$, 74.13 ± 7.37 years old).

2.2. MRI imaging

All MRI images of the selected patients were obtained using the Siemens Aera 1.5T MR. Fat suppression T2-weighted imaging (TR/TE: 5500 ms/100 ms; matrix: 320×320 ; section thickness: 3 mm; field of view: 240×240 mm), T1-weighted imaging (TR/TE: 400 ms/8.6 ms; matrix: 256×256 ; section thickness: 3 mm; field

of view: 240×240 mm), dynamic contrast-enhanced imaging (dose 0.1 mmol/kg standard gadolinium-based contrast agent; injection rate: 3 mL/s), and diffusion-weighted imaging (DWI; TR/TE: 4000/86; matrix: 180×180 ; section thickness: 4 mm; field of view: 240×240 mm; with b-values of 0, 500 s/mm², 1500 s/mm² and 2000 s/mm²) were performed. DKI is a DW image, and we used the two-dimensional spin-echo echoplanar imaging sequence (TR/TE: 4500 ms/92 ms; matrix: 150×150 pixels; slice thickness: 4 mm; acquisition voxel size: $0.9 \times 0.9 \times 4.0$ mm; bandwidth: 1450 Hz/pixel, spectral attenuated inversion recovery fat suppression) in the axial plane. Five averages were chosen for all b-values to maintain a sufficient signal-to-noise ratio. The acquisition time was 6.8 minutes. We used the diffusion gradients in the 12 orthogonal directions, with b-values of 0, 400 s/mm², 800 s/mm², 1200 s/mm² and 2000 s/mm².

2.3. Image analysis

All MRI images were randomly analyzed by a radiologist (10 years of experience in abdominal MRI diagnosis), blinded to the clinical information and outcomes. The Diffusional kurtosis Estimator (Medical University of South Carolina Charleston, version 2.5.1, www.musc.edu/cbi) was used to obtain the mean diffusivity (MD), mean kurtosis (MK), and fractional anisotropy (FA) values from the DKI images. The radiologist reviewed the T1-weighted imaging, T2-weighted imaging, diffusion-weighted imaging, and dynamic contrast-enhanced imaging to determine the location and border of each tumor. Furthermore, transrectal ultrasonography (TRUS)-guided biopsy was combined with the cognitive MRI fusion-guided targeted biopsy to make the one-to-one comparison possible. For each case, the region of interest (ROI) was placed in the largest layer of the lesion to avoid the calcification, urethra and bleeding necrotic area. The ROI was round, and had an area of 25 to 50 mm². The nodular lesions included the entire range, as much as possible, but it did not extend beyond the lesion. If there were more than one lesion, the lesion with the largest diameter was selected for measurement. The diffuse lesions were placed at the maximum level of the ROI in the central zone. Three ROIs were outlined for each lesion, and the average values of the ROIs were calculated. Then, the ROIs were examined by another experienced radiologist.

2.4. PSA test method

The fasting peripheral venous blood was collected for all patients, and the serum was examined. The automatic immunofluorescence detection system (ARCHITECT I2000SR [Abbott Laboratories, USA]) was used to determine the fPSA and total PSA (tPSA) using the fPSA kit and tPSA kit, and calculate the f/t PSA.

2.5. Histopathologic analysis

The histopathologic analysis served as the reference standard for all lesions in the enrolled cohort. Two pathologists with more than eight years of experience performed the analysis. A consensus was resolved by discussion (which involved another pathologist with 10 years of experience) when there was a disagreement. The automatic biopsy gun (GALLIN S.R.L. VPA 18/20) was performed through the 10-point needle biopsy of the prostate, under the guidance of TRUS. Cognitive fusion was employed to determine the exact location for biopsy sampling, following patient MRI review. An urologist performed the biopsy

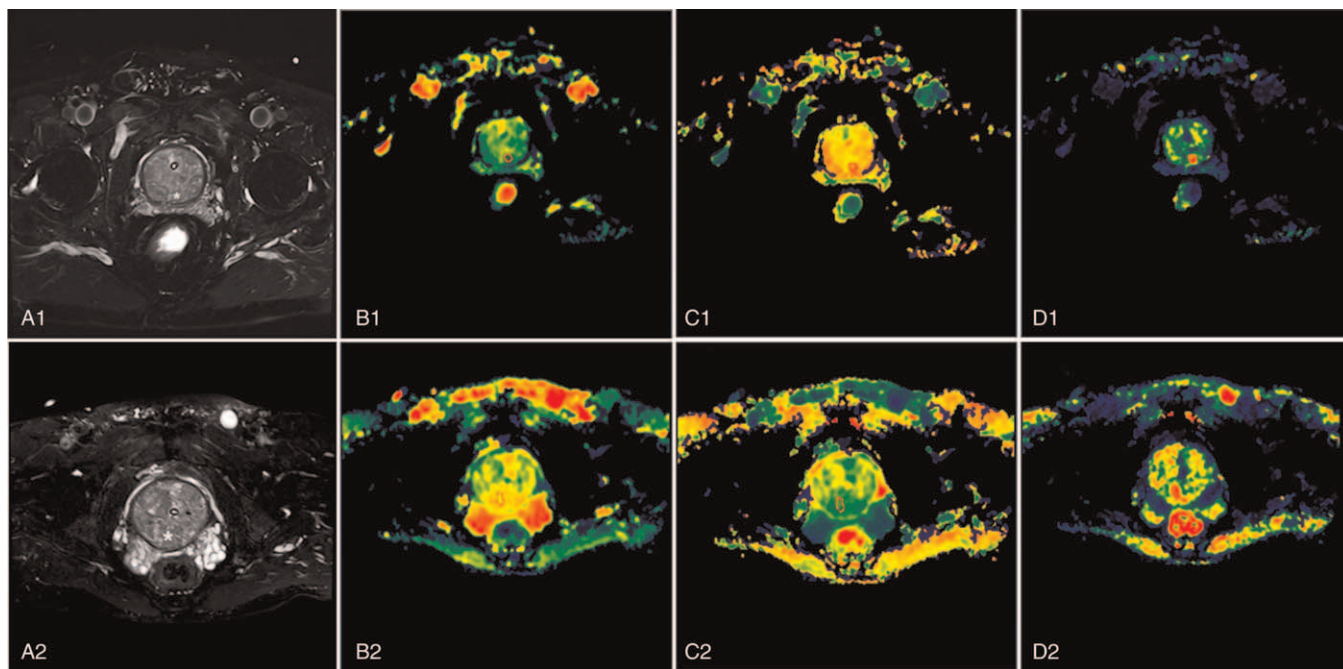


Figure 1. The DKI images, and the corresponding MD, MK, and FA mapping of PCa and BPH in a patient. For the PCa in a 73-year-old male (Gleason score 3+3), the PSA and f/tPSA were 8.15 ng/mL and 0.16, respectively. A1: Axial FS-T2WI, a mixed-signal nodule in the posterior part of the left central zone with blurred boundaries (white asterisks); B1: MD mapping of DKI, the average MD value of the lesion was 1.2177; C1: MK mapping of DKI, the average MK value of the lesion was 1.2073; D1: FA mapping of DKI, the average FA value of the lesion was 0.1407. For the BPH in a 70-year-old male, the PSA and f/tPSA were 6.01 ng/mL and 0.35, respectively. A2: Axial FS-T2WI, a mixed-signal nodule in the posterior part of the central zone, with slightly blurred boundaries (white asterisks); B2: MD mapping of DKI, the average MD value of the lesion was 1.7161; C2: MK mapping of DKI, the average MK value of the lesion was 0.8603; D2: FA mapping of DKI, the average FA value of the lesion was 0.1099. BPH = benign prostatic hyperplasia, DKI = diffusion kurtosis imaging, FA = fractional anisotropy, fPSA = free PSA, MD = mean diffusivity, MK = mean kurtosis, PCa = prostate cancer, PSA = prostate-specific antigen, tPSA = total PSA.

with the assistance of an ultrasonic and radiologist. For patients with no apparent lesion on MRI, a 10+X-G needle under ultrasound guidance will be performed (5 in the peripheral zone, 5 in the transitional zone, X in the suspicious zone).

2.6. Statistical analysis

All statistical analyses were performed with the 0.7 R 3.5.1. The serum and DKI parameters were compared by Student *t* test. Then, the univariate logistic regression analysis was conducted. Factors with a *P*-value of <.05 in the univariate logistic regression analysis were selected to construct the multivariate logistic regression model. This was called, the combined model. The relationship among different parameters and Gleason scores was analyzed by one-way ANOVA, and Kendall tau_b was used to calculate the correlation between the DKI and PSA parameters with the Gleason score. The receiver operating characteristic curves were drawn to determine the performance of the factors and combined model. Then, the accuracy (ACC), area under the curve (AUC), sensitivity (SEN), and specificity (SPE) were calculated. A two-tailed *P*-value of <.05 was considered statistically significant.

3. Results

3.1. General test of the DKI and PSA parameters

A total of 43 patients was enrolled, including 20 cases of BPH and 23 cases of PCa (26.1% (6/23) cases of transition zone PCa).

Among patients with PCa, 26.1% (6/23) had Gleason score 6, 8.7% (2/23) had Gleason score 3+4, 26.1% (6/23) had Gleason score 4+3, and 39.1% (9/23) had Gleason score ≥8. The average size of tumor was 26.81 ± 7.14 mm (range: 8.51–40.60 mm). The examples of DKI parameters of BPH and PCa are shown in Figure 1. The f/t PSA was higher in the BPH group than in the PCa group (0.26 ± 0.09 vs 0.12 ± 0.09, *P* = .001). The PSA value was 9.49 ± 4.81 in the BPH group and 36.57 ± 59.16 in the PCa group, with *P* = .04. The MK value was 0.91 ± 0.17 in the BPH group and 1.21 ± 0.27 in the PCa group, with *P* = .001. Meanwhile, the FA value was 0.10 ± 0.04 in the BPH group and 0.17 ± 0.07 in the PCa group (*P* = .001). There was no significant difference between these two groups in terms of age, fPSA and MD. The details are presented in Table 1.

Table 1
Serum and DKI characteristics in BPH group and PCa group.

	BPH group (N=20)	PCa group (N=23)	<i>P</i>
Age (yr)	68.85 ± 10.81	74.13 ± 7.37	.066
PSA (μg/L)	9.49 ± 4.81	36.57 ± 59.16	.04
fPSA (μg/L)	2.23 ± 1.07	4.12 ± 6.83	.204
f/t PSA	0.26 ± 0.09	0.12 ± 0.09	.001
MD (× 10 ⁻³ s/mm ²)	1.37 ± 0.45	1.22 ± 0.25	.22
MK	0.91 ± 0.17	1.21 ± 0.27	.001
FA	0.10 ± 0.04	0.17 ± 0.07	.001

BPH = benign prostatic hyperplasia, DKI = diffusion kurtosis imaging, FA = fractional anisotropy, fPSA = free PSA, MD = mean diffusivity, MK = mean kurtosis, PCa = prostate cancer, PSA = prostate specific antigen, tPSA = total PSA.

Table 2
Diagnostic performance of DKI and PSA parameters.

	AUC	ACC	SEN	SPE
Age (yr)	0.64	0.628	0.783	0.45
PSA ($\mu\text{g/L}$)	0.69	0.698	0.435	1.00
fPSA ($\mu\text{g/L}$)	0.454	0.581	0.304	0.90
f/t PSA	0.902	0.883	0.87	0.90
MD ($\times 10^{-3}$ s/mm ²)	0.696	0.767	0.913	0.55
MK	0.833	0.791	0.696	0.90
FA	0.807	0.767	0.915	0.55

ACC=Accuracy, AUC=area under the receiver operating characteristic curve, DKI=diffusion kurtosis imaging, FA=graccional anisotropy, fPSA = free PSA, MD=mean diffusivity, MK=mean kurtosis, PSA=prostate specific antigen, SEN=sensitivity, SPE=specificity, tPSA = total PSA.

3.2. Diagnostic performance of DKI and PSA parameters

The diagnostic performance of the DKI and PSA parameters is presented in detail in Table 2. The results show that the AUCs for the f/t PSA, MK, and FA values for diagnosing PCa were 0.902 (95% confidence interval [CI]: 0.801, 1.000), 0.833 (95% CI: 0.707, 0.958), and 0.807 (95% CI: 0.679, 0.934), respectively. The AUC values for the other indicators were < 0.7.

3.3. The correlation of DKI and PSA parameters with the Gleason score

There was no statistical difference between the PSA and Gleason score ($P=.186$), and between the D and Gleason score ($P=.548$). However, there were significant differences between the MK and Gleason score ($P=.001$), and between the FA and Gleason score ($P=.006$). The mean value of MK for the different Gleason score groups (0, 6, 7, 8, and 9) was 0.91, 1.25, 1.12, 1.25, and 1.47, respectively. The mean value of D for the different Gleason score groups was 0.10, 0.15, 0.19, 0.15, and 0.16, respectively. In the nonparametric correlations, the coefficient was 0.270 ($P=.022$) between the PSA and Gleason score, -0.271 ($P=0.021$) between the D and Gleason score, 0.384 ($P=.001$) between the FA and Gleason score, and 0.420 ($P<.001$) between the MK and Gleason score.

3.4. Multivariate logistic regression results

According to the P -value in Table 1, PSA, f/t PSA, MK, and FA were incorporated into the multivariate logistic regression to construct the combined model, in which PSA was not an independent predictor, and the coefficient for f/t PSA, MK, and FA were -24.11 , 9.13 , and 25.44 ($P<.05$), respectively. The expression of the combined model can be expressed, as follows:

Combined model = $-24.11 \times \text{f/t PSA} + 9.13 \times \text{MK} + 25.44 \times \text{FA} - 8.63$.

The AUC, ACC, SEN, and SPE of the combined model, with a cut-off value of 0.475, was 0.972 (95% CI: 0.928, 1.000), 0.930, 0.957, and 0.900, respectively. The receiver operating characteristic curve for f/t PSA, MK, FA, and the combined model are presented in Figure 2. The Delong test revealed that the diagnosis of the combined model was significantly superior to the f/t PSA, MK, and FA model ($P<.05$).

4. Discussion

The present study assessed the potential added value of DKI to serum indicators (PSA, fPSA, and f/t PSA) to distinguish PCa and

BPH using the pathological results of the biopsy guided by TRUS, as reference standards. The DKI parameters (MD, MK, and FA) and f/t PSA can differentiate PCa from BPH. The combined model based on f/tPSA, MK, and FA was developed to quantify the probability of the differential diagnosis of PCa and BPH. The combined model yielded an optimal AUC of 0.972, SEN of 0.957, and SPE of 0.90, which were higher than using f/t PSA, MK, and FA.

Invasive procedures, such as needle biopsy, may be biased due to tumor heterogeneity, and may induce bleeding, and lead to organs injury. Thus, a noninvasive biomarker that can be preoperatively obtained to diagnose PCa and BPH would be valuable in clinical practice. An increasing number of studies have revealed that DKI had good diagnostic performance in differentiating PCa and BPH.^[16–18] DKI is an extension of DWI and diffusion tensor image, which uses a higher b value and multiple diffusion gradient directions, and introduces the 4-order tensor for curve fitting to obtain more accurate quantitative parameters.^[19] Several studies have revealed that DKI findings may be more useful and effective than conventional DWI in detecting PCa, especially MK.^[17,20] The theoretical analysis is that organism water molecules present the gaussian distribution. However, due to the intracellular environment, water molecules tend to a more complex non-Gaussian diffusion mode.^[21] Therefore, conventional DWI evaluation may deviate from the actual state. Furthermore, due to multiple factors, such as necrosis, inflammation, vigorous cell proliferation, and blood vessels, tissue diffusion is more restricted.^[22,23] DKI diffusion coefficient MK reflects the extent of water molecule diffusion that deviates from the Gaussian distribution. Hence, it can effectively reflect the real situation of the diffusion of water molecules in organisms.

Quentin et al^[24] designed the DKI scanning, which was performed in 14 PCa patients and 10 healthy volunteers. The results revealed that the MK value in PCa was significantly higher than that in the normal peripheral and central zones. Meanwhile, DKI parameters were weakly correlated with the Gleason score.^[24] Suo et al^[25] enrolled a total of 19 PCa patients, and performed multi- b -value DWI scanning. The DKI model and single exponential model were used to calculate the MD, apparent diffusion coefficient (ADC), and MK. This revealed that the ADC and MD values of PCa were lower than the benign area, and that the MK value was higher than that in the benign area. The current results are in well agreement with previous studies. The possible reason is that the organization structure of PCa is more complex, which includes the small intercellular space, cell membrane integrity and microcirculation, and real water diffusion is districted by these factors.^[26] Therefore, the MK and FA values were greater, and the MD value was smaller in the PCa group than the BPH group. In the present study, there were statistical differences between these two groups, in terms of MK and FA values. However, there was no statistical difference in MD. The possible reason is the differences in enrolled samples and machines. However, further studies and more samples are needed to verify these results. The present results show that MK and FA in DKI can distinguish PCa from BPH, with an AUC of >0.7. Although some studies have demonstrated that DKI did not improve the PCa detection, because there was no significant difference in the area under the curve of ADC and MK, indicating that MK has a higher sensitivity than ADC.^[17,27]

PSA is a glycoprotein that was first isolated from prostate tissue by immunoprecipitation by Wang et al^[28] in 1979, which

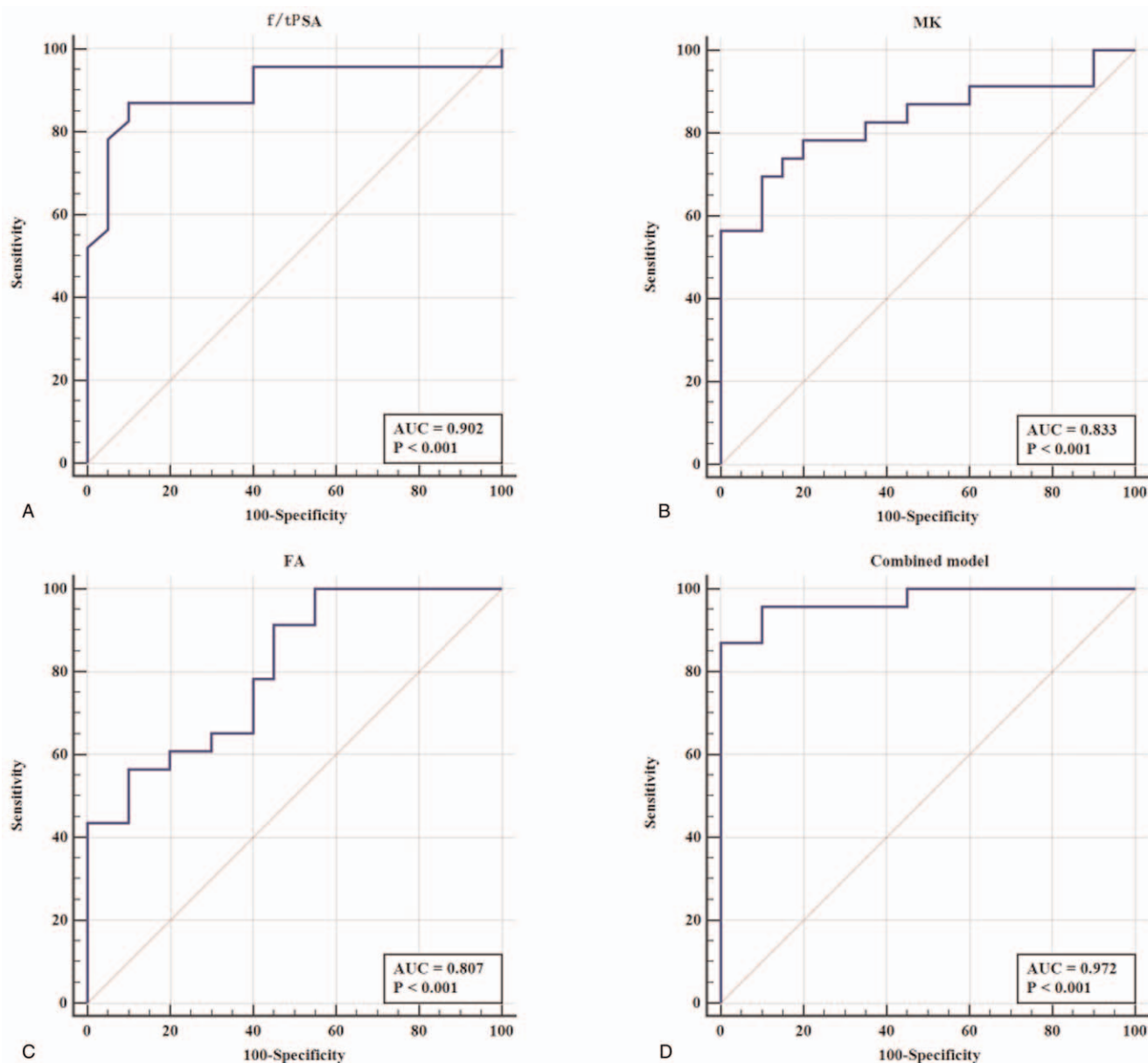


Figure 2. The ROC curve for f/t PSA (A), MK (B), FA (C), and the combined model (D). FA = fractional anisotropy, fPSA = free PSA, MK = mean kurtosis, ROC = receiver operating characteristic, tPSA = total PSA.

remains the best and most widely used tumor marker in urology.^[29] However, PSA is affected by many factors, including age, diet, inflammation, and so on.^[30] PSA is specific for prostate tissues, but not for PCa. PCa, prostatitis, and BPH can all cause the PSA to increase, and there is an overlap between these 3. If the serum tPSA is greater than 4ng/mL, as the prostate biopsy threshold, this will lead to several unnecessary prostate biopsies,^[31] limiting its clinical application. In addition to PSA, other serum indexes should be considered, such as fPSA and f/t PSA, which are often used to improve diagnostic accuracy.^[10] Compared to PSA alone, the f/t PSA combination can increase the specificity of the early detection of PCa.^[32] With the increase in PSA, low f/t PSA is associated with the risk of PCa.^[10] However, the diagnostic performance of f/t PSA is most effective within the PSA range of 4 to 10ng/mL.^[33] The present

study enrolled 23 PCa cases and 20 cases of BPH, we found that the PSA and fPSA in PCa were higher, when compared to the BPH group, and that the f/t PSA in PCa was lower than BPH. However, there was no statistical difference in fPSA level between these 2 groups. The area under curve for f/tPSA was 0.902, with a sensitivity of 0.87 and a specificity of 0.90.

In the present study, there was no statistical significance between PSA and D in the different Gleason groups, but there were significant differences between MK and FA in the different Gleason groups. These findings suggest that MK and FA can be used as quantitative parameters to detect and evaluate the invasiveness of PCa. PCa tissue is characterized by glandular structural destruction and cell proliferation, increased nucleocytoplasmic ratios, and intercellular shrinkage. These microscopic changes represent an increase in organizational complexity.

The non-Gaussian model DKI may be more useful to describe the nuclear inhomogeneity and complexity of the PCa microstructure.

In the present study, at a cutoff of 18.96 $\mu\text{g/L}$ for PSA, the specificity was 1 and the sensitivity was 0.435, which was quite low. A previous study indicated that the combination of PSA, clinical staging, and the Gleason score could predict the pathological stage of PCa.^[34] Since the treatment methods are always selected after comprehensively evaluating the findings of different examinations, the investigators combined different DKI parameters with PSA to further evaluate its predictive value. The combined model of *f/t* PSA, MK, and FA for generating the highest diagnostic performance (AUC=0.972, Accuracy=0.93, Sensitivity=0.957, and Specificity=0.9) indicates that the combination of DKI and serum indicators can improve the diagnostic accuracy of PCa, and decrease unnecessary invasive biopsies. If patients perform DKI and PSA, we can place *f/t* PSA, MK and FA into the combined model formula:

Combined model = $-24.11 \times f/t \text{ PSA} + 9.13 \times \text{MK} + 25.44 \times \text{FA} - 8.63$

If the value of the combined model is greater than the cutoff value (0.475), indicating that the patient has PCa, with an accuracy of 0.93.

There are some limitations to the present study. First, this was a single-center study with a small sample of data, and the results need to be verified through a larger number of data sets. Second, the proportion of PCa and BPH was unbalanced, mainly affected by the actual proportion. Finally, the investigators only used the DKI images. A combination of conventional MRI sequences and DKI should be performed to improve the accuracy of diagnosis performance in future studies.

5. Conclusion

These preliminary results demonstrate that the parameters of DKI may contribute to the diagnosis of PCa and BPH, especially MK and FA. Higher values of MK and FA suggest higher possibilities of PCa. The combination of DKI and serum indicators can further improve the diagnostic capabilities, which may be helpful in distinguishing PCa and BPH earlier, and improved the prognosis of prostate patients.

Acknowledgments

None.

Author contributions

WGY designed and performed most of the experiments and data analysis, and wrote the manuscript. JJZ and CHH contributed to the analysis and interpretation of the data. PCL, LHM, JL, and GCW provided the MRI scan assistance. LFL provided the ultrasound assistance. SFZ provided the needle biopsy assistance. YX provided the pathological assistance.

Conceptualization: Weigen Yao.

Data curation: Weigen Yao, Jiayu Zheng, Chunhong Han.

Formal analysis: Weigen Yao, Jiayu Zheng, Chunhong Han.

Funding acquisition: Weigen Yao.

Investigation: Weigen Yao, Pengcong Lu, Lihua Mao, Jie Liu, GuiCha Wang, Shufang Zou.

Methodology: Weigen Yao, Lifeng Li.

Project administration: Weigen Yao.

Resources: Weigen Yao.

Software: Weigen Yao, Pengcong Lu, Lihua Mao, Jie Liu, GuiCha Wang, Ying Xu.

Supervision: Weigen Yao.

Validation: Weigen Yao.

Visualization: Weigen Yao.

Writing – original draft: Weigen Yao.

Writing – review & editing: Weigen Yao, Chunhong Han.

References

- [1] Zheng Z, Zhou Z, Yan W, et al. Tumor characteristics, treatments, and survival outcomes in prostate cancer patients with a PSA level < 4 ng/ml: a population-based study. *BMC cancer* 2020;20:340.
- [2] Siegel RL, Miller KD, Jemal A. Cancer statistics, 2019. *CA: Cancer J Clin* 2019;69:7–34.
- [3] Wang Y, Wang J, Yan K, Lin J, Zheng Z, Bi J. Identification of core genes associated with prostate cancer progression and outcome via bioinformatics analysis in multiple databases. *PeerJ* 2020;8:e8786.
- [4] Heidenreich A, Bastian PJ, Bellmunt J, et al. EAU guidelines on prostate cancer. Part II: treatment of advanced, relapsing, and castration-resistant prostate cancer. *Eur Urol* 2014;65:467–79.
- [5] Malinowski B, Wiciński M, Musiała N, Osowska I, Szostak M. Previous, Current, and future pharmacotherapy and diagnosis of prostate cancer—a comprehensive review. *Diagnostics (Basel, Switzerland)* 2019;9:161.
- [6] Weinreb JC, Barentsz JO, Choyke PL, et al. PI-RADS prostate imaging - reporting and data system: 2015, Version 2. *Eur Urol* 2016;69:16–40.
- [7] Anastasiadis A, Zapala L, Cordeiro E, Antoniewicz A, Dimitriadis G, De Reijke T. Complications of prostate biopsy. *Exp Rev Anticancer Ther* 2013;13:829–37.
- [8] Thompson IM, Ankerst DP, Chi C, et al. Assessing prostate cancer risk: results from the prostate cancer prevention trial. *J Natl Cancer Inst* 2006;98:529–34.
- [9] Eide IA, Angelsen A. Prostate-specific antigen. *Tidsskr Nor Laegeforen* 2000;120:2528–31.
- [10] Catalona WJ, Southwick PC, Slawin KM, et al. Comparison of percent free PSA, PSA density, and age-specific PSA cutoffs for prostate cancer detection and staging. *Urology* 2000;56:255–60.
- [11] Mendhiratta N, Taneja SS, Rosenkrantz AB. The role of MRI in prostate cancer diagnosis and management. *Future Oncology (London, England)* 2016;12:2431–43.
- [12] Harmon SA, Brown GT, Sanford T, et al. Spatial density and diversity of architectural histology in prostate cancer: influence on diffusion weighted magnetic resonance imaging. *Quant Imaging Med Surg* 2020;10:326–39.
- [13] Gatti M, Faletti R, Callaris G, et al. Prostate cancer detection with biparametric magnetic resonance imaging (bpMRI) by readers with different experience: performance and comparison with multiparametric (mpMRI). *Abdom Radiol (NY)* 2019;44:1883–93.
- [14] Christou A, Ghiatas A, Priovolos D, Veliou K, Bougias H. Accuracy of diffusion kurtosis imaging in characterization of breast lesions. *Br J Radiol* 2017;90:20160873.
- [15] Monti S, Brancato V, Di Costanzo G, et al. Multiparametric MRI for prostate cancer detection: new insights into the combined use of a radiomic approach with advanced acquisition protocol. *Cancers* 2020;12:390.
- [16] Wang Q, Li H, Yan X, et al. Histogram analysis of diffusion kurtosis magnetic resonance imaging in differentiation of pathologic Gleason grade of prostate cancer. *Urol Oncol* 2015;33:337.e315–24.
- [17] Tamura C, Shinmoto H, Soga S, et al. Diffusion kurtosis imaging study of prostate cancer: preliminary findings. *JMRI* 2014;40:723–9.
- [18] Lawrence EM, Warren AY, Priest AN, et al. Evaluating prostate cancer using fractional tissue composition of radical prostatectomy specimens and pre-operative diffusional kurtosis magnetic resonance imaging. *PLoS one* 2016;11:e0159652.
- [19] Marralle M, Collura G, Brai M, et al. Physics, techniques and review of neuroradiological applications of diffusion kurtosis imaging (DKI). *Clin Neuroradiol* 2016;26:391–403.
- [20] Vargas HA, Lawrence EM, Mazaheri Y, Sala E. Updates in advanced diffusion-weighted magnetic resonance imaging techniques in the evaluation of prostate cancer. *World J Radiol* 2015;7:184–8.
- [21] Rosenkrantz AB, Padhani AR, Chenevert TL, et al. Body diffusion kurtosis imaging: basic principles, applications, and considerations for clinical practice. *JMRI* 2015;42:1190–202.

- [22] Cao L, Chen J, Duan T, et al. Diffusion kurtosis imaging (DKI) of hepatocellular carcinoma: correlation with microvascular invasion and histologic grade. *Quant Imaging Med Surg* 2019;9:590–602.
- [23] Payabvash S. Quantitative diffusion magnetic resonance imaging in head and neck tumors. *Quant Imaging Med Surg* 2018;8:1052–65.
- [24] Quentin M, Pentang G, Schimmöller L, et al. Feasibility of diffusional kurtosis tensor imaging in prostate MRI for the assessment of prostate cancer: preliminary results. *Magn Reson Imaging* 2014;32:880–5.
- [25] Suo S, Chen X, Wu L, et al. Non-Gaussian water diffusion kurtosis imaging of prostate cancer. *Magn Reson Imaging* 2014;32:421–7.
- [26] Panagiotaki E, Chan RW, Dikaos N, et al. Microstructural characterization of normal and malignant human prostate tissue with vascular, extracellular, and restricted diffusion for cytometry in tumours magnetic resonance imaging. *Invest Radiol* 2015;50:218–27.
- [27] Roethke MC, Kuder TA, Kuru TH, et al. Evaluation of diffusion kurtosis imaging versus standard diffusion imaging for detection and grading of peripheral zone prostate cancer. *Invest Radiol* 2015;50:483–9.
- [28] Wang MC, Valenzuela LA, Murphy GP, Chu TM. Purification of a human prostate specific antigen. *Invest Urol* 1979;17:159–63.
- [29] Polascik TJ, Oesterling JE, Partin AW. Prostate specific antigen: a decade of discovery—what we have learned and where we are going. *J Urol* 1999;162:293–306.
- [30] Liu ZY, Sun YH, Xu CL, Gao X, Zhang LM, Ren SC. Age-specific PSA reference ranges in Chinese men without prostate cancer. *Asian J Androl* 2009;11:100–3.
- [31] Morote J, Trilla E, Esquena S, et al. The percentage of free prostatic-specific antigen is also useful in men with normal digital rectal examination and serum prostatic-specific antigen between 10.1 and 20 ng/ml. *Eur Urol* 2002;42:333–7.
- [32] Finne P, Auvinen A, Määttänen L, et al. Diagnostic value of free prostate-specific antigen among men with a prostate-specific antigen Level of <3.0 µg per liter. *Eur Urol* 2008;54:362–70.
- [33] Roddam AW, Duffy MJ, Hamdy FC, et al. Use of prostate-specific antigen (PSA) isoforms for the detection of prostate cancer in men with a PSA level of 2–10 ng/ml: systematic review and meta-analysis. *Eur Urol* 2005;48:386–99.
- [34] Graefen M. Combination of prostate-specific antigen, clinical stage, and Gleason score to predict pathological stage of localized prostate cancer—a multi-institutional update. *Aktuelle Urol* 2004;35:377–8.